IEEE Open Access Journal of Power and Energy

Received 18 September 2022; revised 11 January 2023; accepted 19 January 2023.
Date of publication 8 February 2023; date of current version 24 May 2023.

Digital Object Identifier 10.1109/OAJPE.2023.3243385

Revenue Metering of Unbalanced Prosumers in Energy Communities

JAN KLUSACEK[1] (Student Member, IEEE), JIRI DRAPELA[1] (Senior Member, IEEE), AND ROBERTO LANGELLA[2] (Senior Member, IEEE)

[1]Department of Electrical Power Engineering, Faculty of Electrical Engineering and Communication, Brno University of Technology, 61200 Brno, Czech Republic
[2]Department of Engineering, University of Campania Luigi Vanvitelli, 81031 Aversa, Italy
CORRESPONDING AUTHOR: J. KLUSACEK (klusacekj@vut.cz)

This work was supported in part by the Centre for Research and Utilization of Renewable Energy and in part by the Ministry of Education, Youth and Sports of the Czech Republic under Brno University of Technology Specific Research Program under Project FEKT-S-23-8403.

ABSTRACT The presence of power generating plants owned by prosumers may lead to unbalanced bidirectional energy flows at the points of connection to the relevant distribution systems. This will impact future energy communities, where appropriate metering within the community is a crucial issue for billing purposes. This paper shows that the current metrics for active energy measurement and the registration of three-phase revenue meters may fail to fairly charge unbalanced prosumers for their use of the distribution system as an inherent phase-to-phase balancer. On the other hand, it is proven here that adopting metrics based on positive sequence power/energy measurement would lead to more fair billing within the community. A comparative study was performed using a simplified but realistic model of a distribution system feeding two prosumers (i.e., an archetype of an energy community). First, representative case studies were considered. Then, a more realistic simulation of a single day of operation was conducted. The main contribution of the paper is a detailed and systematic comparison of the methods used for measuring and sorting energy into registers in revenue meters to support the ongoing discussions about fair metering within future energy communities.

INDEX TERMS Distribution system utilization, energy community, prosumers, revenue metering, symmetrical components.

I. INTRODUCTION

THE increasing penetration of distributed generation (DG), predominantly in low-voltage (LV) networks, allows energy generation to be closer to energy consumption. This will reduce transmission and distribution losses, as widely accepted and demonstrated, being one of the objectives for energy communities. On the other hand, DG causes bidirectional energy flows that significantly change the paradigm of the energy flow in a distribution system (DS) and affects the energy registration [1], [2], [3]. Furthermore, both the generation and consumption of power may become unbalanced, leading to a voltage imbalance and increased losses in the DS [4], [5], [6], [7], [8].

Historically, the active energy flow was unidirectional and any additional losses due to a power imbalance were tolerated in favor of simplicity, with limits fixed for imbalance indexes [9]. Accordingly, energy registration using revenue meters (RMs) for billing purposes was settled and simplified to obtain a single value of accumulated active energy for a three-phase system.

In this framework, customers became both consumers and producers of energy (i.e., prosumers), with their own energy goals. Moreover, energy communities, consisting of consumers, producers, or prosumers, are becoming an emerging concept to increase the overall efficiency of DSs. This naturally results in bidirectional, unbalanced, and time-varying active energy flows. In the RMs used for bidirectional energy flow measurement, the accumulated active energy is additionally sorted according to the energy flow direction [10]. The registered consumed/generated energy values in RMs are further used for 1) billing the cost of active energy generation in power plants and 2) billing the distribution fees.

Additionally, the power quality criteria, and thus the effectiveness of the energy transfer, might be included and

evaluated: 1) by means of a special quantity (e.g., the reactive power/energy [10] or effective apparent power [11]) or 2) the increase (decrease) in the consumed (generated) energy by values that objectively reflect the corresponding losses. Nevertheless, the bill is considered fair if it reflects the real customer's usage of the DS. For the sake of clarity, the losses in the DS are considered to be one of the objective measures of the grid usage [6].

The imbalance might even be increased with power balancing devices (e.g., a controlled immersion heater and hot water tank), balancing the power at a prosumer point of connection (PoC) and utilizing the excess produced energy intentionally and controllably (e.g., for heating [12], [13]). Studies [14], [15] have shown that customers with inappropriate power balancing may still use the network as an inherent balancer or even accumulator while taking advantage of the active energy measurement and registration metrics in RMs. It can be deduced that with an increasing number of such customers, the standard (consuming only) customers will be billed for the DS operation costs unfairly, as shown in previous studies [2], [3]. Furthermore, the balancing prosumers may contribute to voltage disturbances (typically voltage harmonics, fluctuation [16], and imbalance). Thus, the losses might even be amplified because of their negative effects on other appliances and elements in DSs [17], [18], [19].

The voltage unbalance in DSs were monitored using extensive measurement campaigns in [20] and [21], where the authors commented on the seasonal trends. However, they did not evaluate the energy flows and losses. The authors in [22] focused on a customer's unbalanced contribution in the planning stage of its installation, and they proposed the use of the unbalanced power as a tool for monitoring customers' unbalanced contributions. However, they did not consider the losses either. The additional losses in DSs due to customer unbalance were shown in [6] with reference to a very simple explanatory system (three-phase generator feeding a three-phase resistive load through a three-wire resistive line), proposing for the first time a fair billing method based on power symmetrical components. The authors in [9] demonstrated the same principle applied to prosumers with bidirectional energy flows. However, they did not consider the neutral path. The authors in [23] analyzed the neutral path losses in the context of the apparent power, as defined in [11], showing that the ratio of the neutral current path to the line resistance has a significant impact. The apparent power according to [11] was presented as a quantity reflecting the voltage unbalance. However, the authors in [24] showed that the related power factor penalizes customers with three-phase induction machines.

In [25], a systematic study of a single prosumer with unbalanced generation and consumption connected to a realistically parametrized model of a four-wire DS has been performed for specific cases, while showing the numerical results of the registered energy by standard RM metrics and an RM metric based on power symmetrical components.

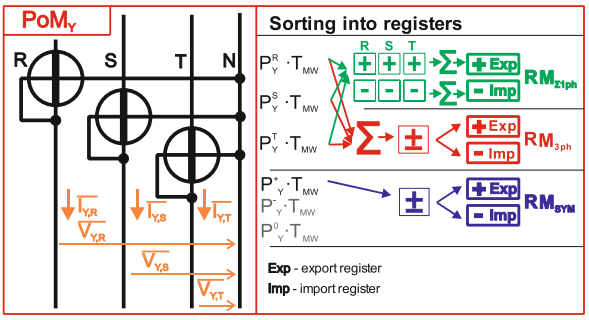

FIGURE 1. Simplified representation of the sorting of measured active energy increments into the three considered revenue meters, where (+) and (–) are the import and export cumulative registers, respectively.

Furthermore, it has been shown that additional losses can be assessed by measuring the negative and zero sequence power at the PoC of a prosumer with a good approximation. This paper extends the previous study [25], primarily by introducing a further prosumer and obtaining a simple and basic case of an energy community using part of the DS. A set of representative unbalanced steady-state cases is analyzed to compare the performances of RM metrics at various points of the DS and how a prosumer might be charged more fairly for using the grid as a balancer when registering positive sequence power/energy. Moreover, the same test system is employed to simulate a representative realistic single day of operation to assess the severity of the deviations between RM metrics in longer-term metering time periods.

II. ACTIVE ENERGY REGISTRATION IN REVENUE METERS

Most of today's smart RMs measure increments of the active single-phase energy that passes through a point of measurement (PoM) in a certain time interval or measuring window (T_{MW}, typically 1 s) [14]. Supposing a three-phase four-wire (3P4W) LV system and a customer connection, three values of energy increments are obtained. Subsequently, the measured energy increments are accumulated, sorted, and summed up into import (Imp, +) or export (Exp,-) registers, based on the sign according to the consumption convention, thus increasing the values in registers by increments of ΔA_{Imp} and/or ΔA_{Exp}.

Three methods of measurement, accumulation, and sorting are shown in Fig. 1, where the subscript Y indicates the specific PoM. The first two methods, $\mathrm{RM}_{\Sigma 1\mathrm{ph}}$ and $\mathrm{RM}_{3\mathrm{ph}}$, are standard methods implemented in current static RMs [14], and the third method, $\mathrm{RM}_{\mathrm{SYM}}$ has been derived from [6] and [9].

The $\mathrm{RM}_{\Sigma 1\mathrm{ph}}$ method sorts each phase energy increment at the end of every T_{MW} first and then accumulates the results individually in corresponding Imp and Exp registers ((1), (2)). Therefore, it is expected to provide information about the total energy transfer (with separate consumption

and generation values) in each T_{MW} at $\mathrm{PoM_Y}$:

$$\Delta A^{\Sigma 1ph}_{Imp,Y} = T_{MW} \cdot \sum_{m=\{R,S,T\}} \left\{ \begin{array}{l} |P^m_Y|, \, if \; P^m_Y > 0 \\ 0, \, if \; P^m_Y \leq 0 \end{array} \right\}, \quad (1)$$

$$\Delta A^{\Sigma 1ph}_{Exp,Y} = T_{MW} \cdot \sum_{m=\{R,S,T\}} \left\{ \begin{array}{l} |P^m_Y|, \, if \; P^m_Y < 0 \\ 0, \, if \; P^m_Y \geq 0 \end{array} \right\}. \quad (2)$$

The second method, $\mathrm{RM_{3ph}}$, arithmetically sums the measured single-phase energy increments first, and then stores the balance result into the corresponding Imp or Exp register depending on its sign ((3), (4)). Thus, it is expected to provide a net energy balance over the phases in each T_{MW} at $\mathrm{PoM_Y}$:

$$\Delta A^{3ph}_{Imp,Y} = T_{MW} \cdot \left\{ \begin{array}{l} \left| \sum_{m=\{R,S,T\}} P^m_Y \right|, \, if \; the \; \Sigma > 0 \\ 0, \, if \; the \; \Sigma \leq 0 \end{array} \right\}, \quad (3)$$

$$\Delta A^{3ph}_{Exp,Y} = T_{MW} \cdot \left\{ \begin{array}{l} \left| \sum_{m=\{R,S,T\}} P^m_Y \right|, \, if \; the \Sigma < 0 \\ 0, \, if \; the \Sigma \geq 0 \end{array} \right\}. \quad (4)$$

Unlike $\mathrm{RM_{3ph}}$ and $\mathrm{RM_{\Sigma 1ph}}$, the third method, $\mathrm{RM_{SYM}}$, is based on positive, negative, and zero sequence power components at $\mathrm{PoM_Y}$ (P^+_Y, P^-_Y, and P^0_Y, respectively):

$$P^+_{\mathrm{Y}} = 3 \cdot |\underline{V}^+_{\mathrm{Y}}| \cdot |\underline{I}^+_{\mathrm{Y}}| \cdot \cos \varphi^+_Y, \quad (5)$$

$$P^-_{\mathrm{Y}} = 3 \cdot |\underline{V}^-_{\mathrm{Y}}| \cdot |\underline{I}^-_{\mathrm{Y}}| \cdot \cos \varphi^-_Y, \quad (6)$$

$$P^0_{\mathrm{Y}} = 3 \cdot |\underline{V}^0_{\mathrm{Y}}| \cdot |\underline{I}^0_{\mathrm{Y}}| \cdot \cos \varphi^0_Y. \quad (7)$$

where the positive, negative, and zero sequence voltage and current components ($\underline{V}^+_{\mathrm{Y}}$, $\underline{V}^-_{\mathrm{Y}}$, $\underline{V}^0_{\mathrm{Y}}$, $\underline{I}^+_{\mathrm{Y}}$, $\underline{I}^-_{\mathrm{Y}}$, and $\underline{I}^0_{\mathrm{Y}}$, respectively) are phasors obtained using the Fortescue transform. The energy increment of the positive sequence is stored in either the Imp or Exp register ((8), (9)) in each T_{MW} at $\mathrm{PoM_Y}$:

$$\Delta A^{SYM}_{Imp,Y} = T_{MW} \cdot \left\{ \begin{array}{l} \left| P^+_Y \right|, \, if \; P^+_Y > 0 \\ 0, \, if \; P^+_Y \leq 0 \end{array} \right\}, \quad (8)$$

$$\Delta A^{SYM}_{Exp,Y} = T_{MW} \cdot \left\{ \begin{array}{l} \left| P^+_Y \right|, \, if \; P^+_Y < 0 \\ 0, \, if \; P^+_Y \geq 0 \end{array} \right\}. \quad (9)$$

The $\mathrm{RM_{SYM}}$ method was recognized as a fair approach for energy measurement and registration in [6] and [9]. It has been demonstrated that the method naturally accounts for the additional energy required to compensate the voltage and current unbalances to absorb (generate) the same active power that the prosumer would absorb (generate) under balanced conditions; consequently, it naturally penalizes the unbalancing customers. Obviously, under balanced conditions, the $\mathrm{RM_{SYM}}$ method converges to the same results provided by $\mathrm{RM_{3ph}}$ and $\mathrm{RM_{\Sigma 1ph}}$.

Because the active energy increment accumulated in time interval T_{MW} is equivalent to the average active power over this interval, the active power is used for the investigation of the sorting into registers in the following parts of the paper.

III. ADDITIONAL LOSSES DUE TO UNBALANCE

As mentioned in the introduction, the author in [6] demonstrated that unbalanced customers produce additional losses (ΔP_{add}) in the distribution grid compared to the losses (ΔP_{bal}) produced by an equivalent balanced load absorbing the same active power but distributed evenly across the three phases (balanced state):

$$\Delta P_{add} = \Delta P_{act} - \Delta P_{bal} = \Delta P^- + \Delta P^0 + \Delta P_{HID}, \quad (10)$$

where ΔP_{act} is the actual total losses in the system; ΔP^- and ΔP^0 are the losses produced by the negative and zero power symmetrical components, respectively; and ΔP_{HID} is the so-called hidden power.

A. HIDDEN POWER

The origin of the hidden power was explained in [6] as related to the increment of the positive sequence power required for the generator to feed the unbalanced load, which is converted into negative and zero sequence power values. Later, ΔP_{HID} is also called the hidden loss because of its nature in the context of a DS. The author of [6] pointed out that the quantity of ΔP_{HID} cannot be detected from a measurement at the load terminals (i.e., PoC).

B. ESTIMATION OF ADDITIONAL LOSSES DUE TO UNBALANCE

Additional losses can be practically estimated by multiplying the summed absolute values of P^0_Y and P^-_Y measured at a specific $\mathrm{PoM_Y}$ by a coefficient, K_{PI}, which reflects the hidden losses (which cannot be directly measured). Therefore, (10) can be rewritten as follows:

$$\begin{aligned} \Delta P_{add} &= \Delta P_{act} - \Delta P_{bal} = \Delta P^- + \Delta P^0 + \Delta P^+ - \Delta P_{bal} \\ &= \Delta P^- + \Delta P^0 + \Delta P_{HID} \\ &\approx \left(\left| P^-_Y \right| + \left| P^0_Y \right| \right) \cdot K_{PI}, \end{aligned} \quad (11)$$

where ΔP^+ is the loss produced by the positive power symmetrical component. For analytical purposes, K_{PI} is expressed as in (11) based on the following assumptions: i) ΔP_{act} and ΔP_{bal} are known and ii) P^0_Y and P^-_Y are measured:

$$K_{PI} = \frac{\Delta P_{act} - \Delta P_{bal}}{|P^-_Y| + |P^0_Y|} = \frac{\Delta P^- + \Delta P^0 + |\Delta P^+ - \Delta P_{bal}|}{|P^-_Y| + |P^0_Y|}. \quad (12)$$

It should be noted that the difference $|\Delta P^+ - \Delta P_{bal}|$ is an absolute value to prevent anticipating the responsibility for ΔP_{HID} at this stage. Additionally, in (13) and 14, K_{PI} is presented as a function of symmetrical components of the current measured at PoC (I^+_Y, I^-_Y, and I^0_Y), positive sequence current of the corresponding balanced state (I_{bal}), and grid

resistance ratio R_N/R_L:

$$K_{PI} = \frac{3R_L(I_Y^-)^2 + 3R_L(I_Y^0)^2 + R_N(3I_Y^0)^2 + |3R_L(I_Y^+)^2 - 3R_L(I_{bal})^2|}{3R_L(I_Y^-)^2 + 3R_L(I_Y^0)^2 + R_N\left(3I_Y^0\right)^2} \tag{13}$$

$$K_{PI} = 1 + \frac{|(I_Y^+)^2 - (I_{bal})^2|}{(I_Y^-)^2 + (I_Y^0)^2\left(1 + 3\frac{R_N}{R_L}\right)}. \tag{14}$$

It is important to note that the terms I_Y^+, I_Y^-, and I_Y^0 indicate the prosumer' state (i.e., its working point), and grid resistance ratio R_N/R_L is a design factor for the grid. It is straightforward to note that the index is invariant to absolute values of R_L and R_N. Generally, the R_N/R_L ratio is not known at the PoC. Typical values might be used for estimation purposes instead.

C. UNBALANCE LEVEL QUANTIFICATION – "PROSUMITY" INDEX

To quantify a prosumer's state by means of its power distribution into the phases with respect to the demand or supply using a single numerical value, the "prosumity" index (PI) is introduced. The PI fulfills two conditions: i) it is defined using measurable quantities, and ii) its value falls within a closed interval (e.g., -1:1):

$$PI = \frac{P_Y^+}{|P_Y^+| + |P_Y^-| + |P_Y^0|}. \tag{15}$$

IV. TEST SYSTEM

To analyze the additional losses due to unbalance and examine the ability of RM metrics to fairly detect them, the steady-state model of a 3P4W DS serving two prosumers is implemented, as shown in Fig. 2.

The prosumers (PRO1 and PRO2) are connected to a point of common connection (PCC) via their own PoCs, which is supplied from the utility feeder (FEED). The feeder is modeled as an ideal AC 50 Hz 3-phase 4-wire voltage source, with a line-to-neutral rated voltage of 230 V. The whole network impedance is assumed to be the LV reference impedance [28], typically characterizing the 75th–95th percentile of connection impedances at all LV PoCs: $\underline{Z}_L = (0.24 + j0.15)\ \Omega$, and $\underline{Z}_N = (0.16 + j0.10)\ \Omega$. Next, the reference impedance is attributed to 1/3 of the feeder impedance at the PCC and 2/3 from the PCC to each PoC. The 1/3 division is selected to observe the disturbances at the PCC caused by the unbalanced prosumers with adequate resolution. Moreover, the remaining part of the reference impedance (2/3 of $\underline{Z}_L$ and $\underline{Z}_N$) reflects the fact that 60% of the losses in the DS are dissipated in the LV part.

Furthermore, six red-marked PoMs are indicated, three at the PCC (FEED,PCC; PRO1,PCC; and PRO2,PCC) and three at each PoC (FEED,PoC; PRO1,PoC; and PRO2,PoC). The

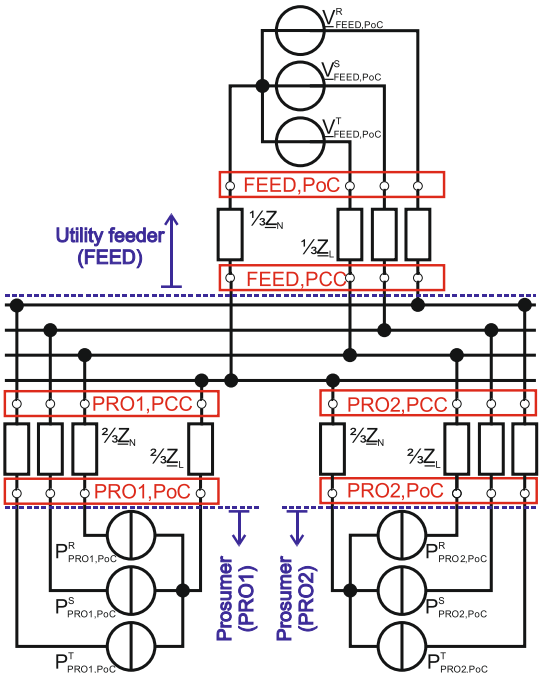

FIGURE 2. Test power grid (3P4W) and prosumer model for analysis.

phase voltages, $\underline{V}_Y^X$, and currents, $\underline{I}_Y^X (X \in \{R, S, T\})$, are recorded for all the calculations in the post-processing stage.

The desired energy flow at the prosumer's PoC is forced by means of controlled current sources providing active power P_Y^X to the phase, $X \in \{R, S, T\}$, at point $Y \in \{PRO1,PoC; PRO2,PoC\}$. The value of P_Y^X is the resulting arithmetic sum of the active power values of the generators ($P_{Y,gen}^X$) and loads ($P_{Y,load}^X$) within the prosumer's installation at its PoC at phase X. Moreover, the total power can be set as a power function of the voltage magnitude, V_Y^X:

$$P_Y^X = \left(P_{Y,gen}^X + P_{Y,load}^X\right) \cdot \left(\frac{V_Y^X}{V_n}\right)^k, \tag{16}$$

where V_n is the rated voltage, and exponent k is practically in the range (0:2), e.g., $k = 0$, 1 or 2 for constant power, constant current, or constant resistance, respectively. The power factor is assumed to be equal to one, for the sake of simplicity and clarity, unless defined otherwise.

The model is implemented in MATLAB Simulink, and the phasor solution method is used to perform (even consecutive) steady state simulations on the fundamental frequency.

In what follows, the active power (W) is used when describing a single steady state, whereas the energy (kWh) is used in the description of a sequence of steady states.

V. SINGLE PROSUMER

The analysis of the energy flow in a system with a single prosumer (PRO2) connected to the feeder (FEED,PoC) via impedances $\underline{Z}_L$ and $\underline{Z}_N$ is performed using six specific base

TABLE 1. Single prosumer simulation results (Y = PRO2,PoC).

		Case 1 (BC)	Case 2 (BG)	Case 3 (UC)	Case 4 (UG)	Case 5 ($CB_{\Sigma 0}$)	Case 6 (CB_{POS0})
P_Y^R (W)		1227	-1227	3680	0	1840	1810
P_Y^S (W)		1227	-1227	0	-3680	-1840	-1870
P_Y^T (W)		1227	-1227	0	0	0	0
P_Y^+ (W)		3680.0	-3680.0	3766.9	-3602.3	60.8	0.0
P_Y^- (W)		0.0	0.0	-21.7	-19.4	-15.5	-15.5
P_Y^0 (W)		0.0	0.0	-65.1	-58.3	-45.3	-45.3
ΔP_{act} (W)		20.71	20.26	108.57	97.10	60.78	60.71
ΔP_{bal} (W)		20.71	20.26	20.71	20.26	0.00	0.01
ΔP_{add} (W)		0.00	0.00	87.85	76.84	60.78	60.70
ΔP_{HD} (W)		0.00	0.00	1.00	0.84	0.01	0.00
$P_Y^{\Sigma 1ph}$ (W)	Exp	3680	0	3680	0	1840	1810
	Imp	0	-3680	0	-3680	-1840	-1870
P_Y^{3ph} (W)	Exp	3680	0	3680	0	0	0
	Imp	0	-3680	0	-3680	0	-61
P_Y^{SYM} (W)	Exp	3680	0	3767	0	61	0
	Imp	0	-3680	0	-3602	0	0

steady states at PRO2 PoC first, and then generalized to all its possible but rational states under specific assumptions.

A. BASE STATES

The base steady states represent "extreme" exemplary conditions intended to show how the RMs' metrics perform in relation to the network losses when the prosumer absorbs, injects, or exchanges the same power under balanced or unbalanced conditions. Therefore, the sum of the absolute active power values over phases absorbed or injected into the grid at PRO2,PoC is kept constant at the value of 3.68 kW ([1]), which also means $k = 0$ in (16). Six specific cases are designed in total.

The first two cases, Case 1 and Case 2 depicted in Fig. 3 and Fig. 4, respectively, refer to balanced consumption (BC) and generation (BG), and they are considered as reference states as the ideal method for energy transfer in a three-phase DS. Case 3 (Fig. 5) and Case 4 (Fig. 6) refer to consumption and generation on a single phase only (UC and UG, respectively), and they represent standard customers with single-phase connections to the DS. Case 5 (Fig. 7) and Case 6 (Fig. 8) refer to generation in phase R balanced by consumption in phase S to keep the simple energy balance of the 3-ph system at PRO2,PoC equal to zero ($CB_{\Sigma 0}$) and to keep the positive sequence power at PoC equal to zero (CB_{POS0}), respectively. $CB_{\Sigma 0}$ represents the control target of some commercial energy diverters ([13]), while CB_{POS0} intends to present the attributes of an alternative energy management control target (i.e., $P_Y^+ = 0$).

The results measured at the PoC of the prosumer (Y = PRO2,PoC) are reported in TABLE 1., where $P_Y^{\Sigma 1ph}$, P_Y^{3ph}, and P_Y^{SYM} are the active power values measured at PRO2,PoC by $RM_{\Sigma 1ph}$, RM_{3ph}, and RM_{SYM}, respectively. Additionally, Fig. 3–Fig. 8 show the energy flow diagrams [6], together with the current phasors at PRO2,PoC, for the six base cases.

The power flow diagrams shown in Fig. 3 and Fig. 4 (numerically in TABLE 1.) demonstrate that in the balanced states, the system losses, ΔP_{act}, are compensated by the feeder (BC) or prosumer (BG). P_Y^- and P_Y^0 are equal to zero,

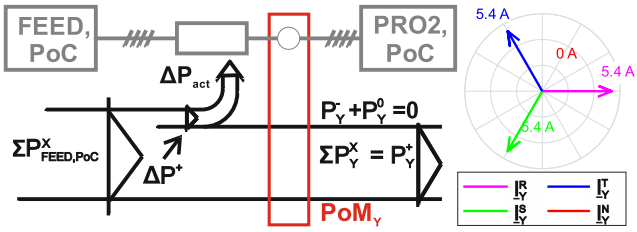

FIGURE 3. Case 1: Balanced consumption (BC), Y = PRO2,PoC.

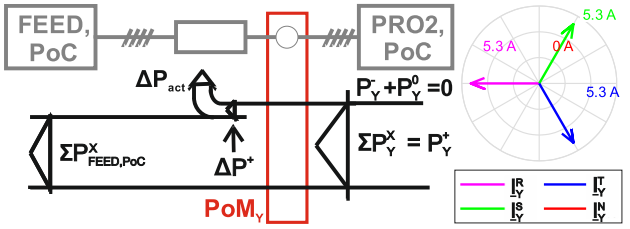

FIGURE 4. Case 2: Balanced generation (BG), Y = PRO2,PoC.

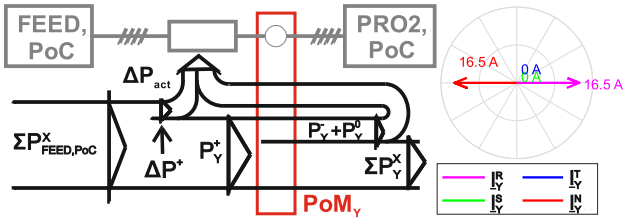

FIGURE 5. Case 3: Single-phase unbalanced consumption (UC), Y = PRO2,PoC.

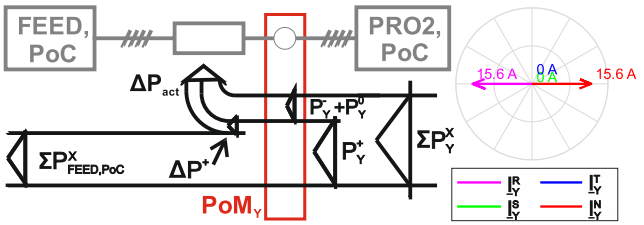

FIGURE 6. Case 4: Single-phase unbalanced generation (UG), Y = PRO2,PoC.

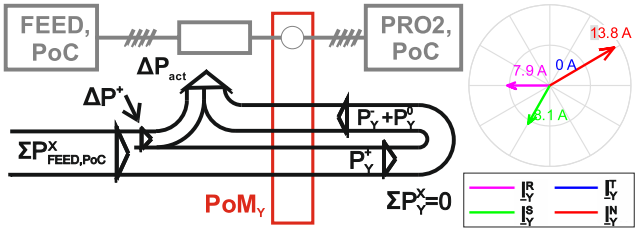

FIGURE 7. Case 5: Generation in R-phase balanced by consumption in S-phase to keep the power sum at PoM zero ($CB_{\Sigma 0}$), Y = PRO2,PoC.

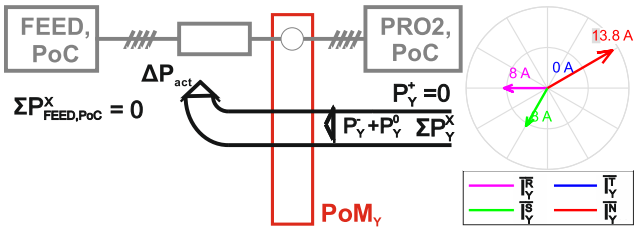

FIGURE 8. Case 6: Generation in R-phase balanced by consumption in S-phase to keep the positive sequence power at PoM zero (CB_{POS0}), Y = PRO2,PoC.

and the losses, ΔP_{act}, cannot be measured at the prosumer PoC. The absolute values of the current consumed/delivered from/to the supply system differ at BC compared to BG as a result of the abovementioned hypothesis of constant power (3.68 kW), which produces voltage drops with altering signs across the grid impedances.

The diagram in Fig. 7 for $CB_{\Sigma 0}$ shows that although the value of P_Y^{3ph} at the prosumer's PoC is zero, the prosumer contributes to the system losses, ΔP_{act}, and they are compensated from the feeder. The value of P_Y^{3ph} is zero in both registers, thus describing only the prosumer's energy balance. In contrast $P_Y^{\Sigma 1ph}$ registers energy in both directions, thus indicating the unbalanced system occupancy. The P_Y^{SYM} measurement result in the import register ($CB_{\Sigma 0}$) is equal to the losses in the network (ΔP_{act}). Thus, RM_{SYM} properly accounts for the actual losses incurred in the system due to the unbalanced operation.

Fig. 5 and Fig. 6 show the power flows in the cases of UC and UG, respectively. P_Y^- and P_Y^0 are dissipated in the DS, and ΔP_{act} is higher in UC and UG than in BC and BG. One may notice in TABLE 1. that the values of P_Y^+ at UC and UG are related to the losses in the system (ΔP_{act}). Consequently, the absolute value of P_Y^{SYM} is higher than $P_Y^{\Sigma 1ph}$ or P_Y^{3ph} in the import register under UC and lower in the export register under UG, i.e., the metric fairly accounts for induced additional losses. This can also be seen from the power flow diagrams.

The power flow diagram in Fig. 8 shows that if the value of ΣP_Y^X at the prosumer's PoC is equal to P_Y^- and P_Y^0, the prosumer is generating the same losses as it induces. It is directly demonstrated by means of CB_{POS0} that if the power is counter-balanced at the PoC to keep the value of P_Y^+ at the PoC zero, the losses due to the imbalanced prosumer are covered by his own generator.

Therefore, the RM_{SYM} metric naturally motivates the prosumer to have fair behavior when targeting a zero energy flow at the PoC. Finally, TABLE 2. reports the values of PI and K_{PI} for the six base cases discussed in section V

It is possible to observe the following:

- in Case 3 (Case 4), the exact amount of the additional losses due to the imbalance is obtained by decreasing (increasing) the result of the direct measurement at the PoC (i.e., $|P_Y^0| + |P_Y^-|$) by 1 %;
- in Case 6, the result of the direct measurement at the PoC (i.e., $|P_Y^0| + |P_Y^-|$) gives exactly the additional losses due to unbalance.

TABLE 2. PI and K_{PI} indexes for the 6 base cases.

	Case 1 (BC)	Case 2 (BG)	Case 3 (UC)	Case 4 (UG)	Case 5 ($CB_{\Sigma 0}$)	Case 6 (CB_{POS0})
PI (-)	1.00	-1.00	0.98	-0.98	0.50	0.00
K_{PI} (-)	NaN	NaN	1.01	0.99	1.00	1.00

TABLE 3. Model's parameters.

Parameter	Value	Comment
Single-phase power threshold rated at 230 V (W or VA)	3680	Corresponds to current per phase of 16A [26]
	4600	Corresponds to current per phase of 20A [27]
	6000	Corresponds to maximal power unbalance in IT [9]
	9200	Corresponds to assumed max current per phase of 40A
$\underline{Z}_L$ (Ω)	0.13+0.09	80th percentile in Switzerland (CH), [28]*
	0.19+0.13	80th percentile in Germany (GE), [28]*
	0.24+j0.16	Reference value acc. to [28]
	0.41+0.27	80th percentile in Czechia (CZ), [28]*
	0.49+0.33	80th percentile in Austria (AT), [28]*
$\underline{Z}_N/\underline{Z}_L$ (-)	0.5; **2/3**; 1; 2	Typical $\underline{Z}_N/\underline{Z}_L$ ratios in LV networks (2/3 in [28])

*The line resistances are calculated from the short-circuit power in [28], assuming an *R/X* ratio of 3/2 [28].

B. ALL POSSIBLE STATES

The previous subsection only focused on six ''extreme'' states of the prosumer, allowing a quantitative examination of the considered RM metrics under unbalanced conditions in relation to the DS utilization. In the following, the range of a single prosumer state (PRO2 in Fig. 2) under 3-phase DS loading is extended to all reasonable scenarios of power at PRO2,PoC to generalize the analysis of the examined metrics' performances.

The considered range of active power is up to 9200 W (40 A) per phase in both directions with steps of 920 W, while involving some possible values for a single-phase power threshold, which are reported in the literature and national grid codes (TABLE 3.). The whole feeder-to-prosumer impedance is selected to be $\underline{Z}_L = (0.24+j16)\ \Omega$, $\underline{Z}_N/\underline{Z}_L = 2/3$. The results obtained for PRO2,PoC, exclusively comparing the performances of the RM_{3ph} and RM_{SYM} metrics, are visualized in the coordinates of each phase of the active power in Fig. 9.

In Fig. 9, each black dot represents the prosumer's operating point (i.e., state), and the red dots on the main diagonal represent the states corresponding to the perfect balanced cases. The surfaces represent sets of states for which the metrics register the same specific value (planar for RM_{3ph} and curved for RM_{SYM}).

The distance between the blue plane ($P_Y^R + P_Y^S + P_Y^T = 0$) and green curved surface ($P_Y^+ = 0$) clearly visualizes the additional losses due to the imbalance; the distances increase

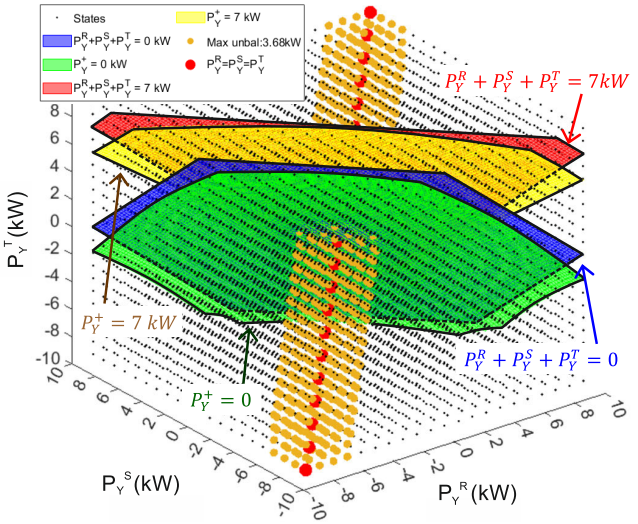

FIGURE 9. **3D representation of the prosumer's states in domain of P_Y^R, P_Y^S, P_Y^T.**

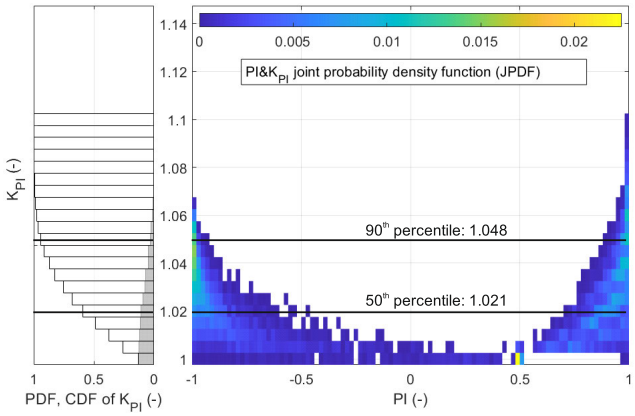

FIGURE 10. **Distribution of K_{PI} in the test network, all states of the cube at PoC can occur with the same probability.**

nonlinearly with the distance from the main diagonal. Nevertheless, the operating range limiting excessive losses can be practically limited by means of the maximal absolute difference between the power values for any of the phases (orange dots in Fig. 9: 3.68 kW limit), as similarly introduced in some countries [27]. The same trend can be recognized for the red plane ($P_Y^R + P_Y^S + P_Y^T = 7$kW) and corresponding yellow surface ($P_Y^+ = 7$kW).

C. UNFAIRNESS RESULTING FROM METERING

As stated above, the distance between the blue (red) plane and green (yellow) surface in Fig. 9 quantifies the difference in the performances of the two examined metrics (because of additional losses due to unbalance). In other words, it is a measure of the unfairness of the RM_{3ph} metric. More seriously, if a prosumer with a deployed RM_{3ph} meter registers zero energy increments (blue plane of Fig. 9 and $CB_{\Sigma 0}$ in TABLE 1.), they are not assuming the financial responsibility for employing the DS at all. It can be deduced that if the ratio of the customers on the blue plane (prosumers intentionally balancing) increases over those on the red plane (e.g., standard customers with consumption only), the unfairness of cost sharing can become severe, especially in local distribution networks, or even in a community sub-grid. The severity of the problem is considered in a case study with two prosumers in the following sections.

D. STATISTICAL DISTRIBUTION OF K_{PI}

Although the K_{PI} index is close to 1 in the six specific states of section V-A (the hidden power is relatively negligible compared to the absolute sum of the power at the PoC), an analysis of its values corresponding to the states represented in Fig. 9 is performed to realistically investigate the significance of K_{PI} in the grids, because it could not be directly measured. The prosumer is studied in the same states as in section V-B However, in combination with all the typical values of $\underline{Z}_L$ and the $\underline{Z}_N/\underline{Z}_L$ ratio, according to TABLE 3. assumed that all the states occurred with the same probability.

The statistical distribution of K_{PI} is depicted in Fig. 10. It can be observed that K_{PI} reaches values from 1.00 to 1.05 in 90% of the states (see PDF and CDF of the K_{PI}), while PI has a range of -1:1, with a significant concentration around a value of 0.5. In the remaining 10% of the states, K_{PI} goes from 1.05 up to 1.10, but the amount of total losses decreases at the same time [25].

Generally, it can be concluded that the K_{PI} range is practically from 1 to 1.05. This means, for example, that measuring $|P_Y^-|$ and $|P_Y^0|$ at the PoC and multiplying their sum by the median value of 1.02 would provide a good approximation of the additional losses due to an unbalanced prosumer.

VI. TWO PROSUMERS

The model in Fig. 2 practically represents a simplified system with three parties: two prosumers (PRO1 and PRO2) connected through part of the LV DS (e.g., a community sub-grid) to a utility feeder (FEED). This section discusses the results if the RMs (Fig. 1) are deployed: i) at the prosumers' PoCs (nodes PRO1,PoC and PRO2,PoC in Fig. 2) and ii) between the utility and community sub-grid (node FEED,PCC in Fig. 2). The system is analyzed in five suitably chosen representative states, Case 7–Case 11. The main objective is to analyze the energy exchange between the two prosumers and the feeder, while observing the ''fairness'' of the energy/power measured by the examined RMs' metrics in terms of extra losses in the DS due to any unbalance.

A. REPRESENTATIVE STATES

Case 7 corresponds to the state where PRO1 symmetrically absorbs exactly the power (3.68 kW) that PRO2 symmetrically generates, thus representing one of the ideal states for

TABLE 4. Two prosumers on adjacent branches.

		Case 7	Case 8	Case 9	Case 10	Case 11
PoM		Y = PRO1,PoC (Prosumer 1)				
P_Y^R (W)		1226.7	3680.0	3680.0	1840.0	1840.0
P_Y^S (W)		1226.7	0.0	0.0	-1840.0	-1840.0
P_Y^T (W)		1226.7	0.0	0.0	0.0	0.0
P_Y^+ (W)		3680.1	3738.2	3772.3	40.7	60.9
$P_Y^- + P_Y^0$ (W)		0.0	-58.2	-92.3	-40.7	-60.9
$P_Y^{\Sigma 1ph}$ (W)	Imp	3680.1	3680.0	3680.0	1840.0	1840.0
	Exp	0.0	0.0	0.0	-1840.0	-1840.0
P_Y^{3ph} (W)	Imp	3680.1	3680.0	3680.0	0.0	0.0
	Exp	0.0	0.0	0.0	0.0	0.0
P_Y^{SYM} (W)	Imp	3680.1	3738.2	3772.3	40.7	60.9
	Exp	0.0	0.0	0.0	0.0	0.0
PoM		Y = PRO2,PoC (Prosumer 2)				
P_Y^R (W)		-1226.7	-3680.0	0.0	-1840.0	1201.8
P_Y^S (W)		-1226.7	0.0	-3680.0	1840.0	1228.8
P_Y^T (W)		-1226.7	0.0	0.0	0.0	1208.6
P_Y^+ (W)		-3680.1	-3628.7	-3582.0	41.3	3639.1
$P_Y^- + P_Y^0$ (W)		0.0	-51.3	-98.0	-41.3	0.1
$P_Y^{\Sigma 1ph}$ (W)	Imp	0.0	0.0	0.0	1840.0	3639.2
	Exp	-3680.1	-3680.0	-3680.0	-1840.0	0.0
P_Y^{3ph} (W)	Imp	0.0	0.0	0.0	0.0	3639.2
	Exp	-3680.1	-3680.0	-3680.0	0.0	0.0
P_Y^{SYM} (W)	Imp	0.0	0.0	0.0	41.3	3639.1
	Exp	-3680.1	-3628.7	-3582.0	0.0	0.0
PoM		Y = FEED,PCC (Utility feeder)				
$P_Y^{\Sigma 1ph}$ (W)	Imp	27.3	136.9	3752.3	82.0	4276.5
	Exp	0.0	0.0	-3615.8	0.0	-583.1
P_Y^{3ph} (W)	Imp	27.3	136.9	136.6	82.0	3693.4
	Exp	0.0	0.0	0.0	0.0	0.0
P_Y^{SYM} (W)	Imp	27.3	137.0	217.6	82.0	3713.6
	Exp	0.0	0.0	0.0	0.0	0.0
ΔP_{act} (W)		27.3	137.0	217.6	82.0	81.3

energy exchange in the community sub-grid and serving as a reference. Case 8 corresponds to the situation where PRO1 absorbs from phase R (3.68 kW) exactly the power that PRO2 generates on the same phase R. In contrast, in Case 9, PRO1 absorbs from phase R the same power that PRO2 generates on phase S. Case 10 corresponds to the situation where PRO1 absorbs from phase R (1.84 kW) the same power generated on phase S, while PRO2, in contrast, absorbs 1.84 kW on phase S, which is the power generated on phase R. Case 11 corresponds to the case where PRO1 consumes on R and generates on S the same power (1.84 kW) as in the previous case, while PRO2 uses a 3-phase balanced passive resistive load ($k = 2$ in (16)) to absorb the nominal 3-phase power of 3.68 kW at the rated voltage (230 V).

B. NUMERICAL RESULTS

The results of an analysis of prosumers on adjacent branches for individual cases are summarized in TABLE 1.

In Case 7, the energy is exchanged between the prosumers symmetrically, and the losses in the community sub-grid (practically almost equal to the total grid losses) are compensated by the utility feeder, which is registered correctly by all the metrics at FEED,PCC ($P^{\Sigma 1ph}_{FEED,PCC} = P^{3ph}_{FEED,PCC} = P^{SYM}_{FEED,PCC}$).

In Case 8, $\mathrm{RM}_{\Sigma 1ph}$ and $\mathrm{RM}_{3\mathrm{ph}}$ both register the same values ($P_Y^{\Sigma 1ph}$ and P_Y^{3ph}, respectively) in the import register of the consuming prosumer (Y = PRO1,PoC) and in the export register of the generating prosumer (Y = PRO2,PoC). This is because of the unidirectional flow at each prosumer PoC, even if unbalanced. Because the energy exchange between the prosumers matches ($P^R_{PRO1,PoC} = P^R_{PRO2,PoC}$), both the standard metrics in the node FEED,PCC register that the energy imported from the utility feeder again cover the present losses in the community sub-grid. $\mathrm{RM}_{\mathrm{SYM}}$ at FEED,PCC registers the energy imported from the utility feeder ($P^{SYM}_{FEED,PCC}$), which represents the total losses in the grid and includes additional losses due to the imbalance, significantly belonging to the community sub-grid. The $\mathrm{RM}_{\mathrm{SYM}}$ metric at the prosumers' PoCs naturally penalizes both the prosumers for their unbalanced power by raising or reducing the $P^{SYM}_{PRO1,PoC}$ or $P^{SYM}_{PRO2,PoC}$ absolute value contributing to the import or export register, respectively. The additional losses accounted to each prosumer are correctly predicted by negative and zero sequence power values. The absolute total additional losses significantly contribute to the total actual losses of Case 8 in respect to Case 7.

In Case 9, $\mathrm{RM}_{\Sigma 1\mathrm{ph}}$ and $\mathrm{RM}_{3\mathrm{ph}}$ register the same energy as in Case 8 at the prosumers' PoCs. However, at node FEED,PCC, the contrast between the values in the Imp and Exp registers of $\mathrm{RM}_{\Sigma 1\mathrm{ph}}$ indicates a higher total power unbalance for the sub-grid. The utility feeder obviously serves as an interphase balancer. Thus, the losses in the network and utility feeder system, compared to Case 8, are higher and result in a much higher ΔP_{act}. Morover, one can notice that the system losses in Case 9 are eight times higher than those in reference Case 7. The $\mathrm{RM}_{\mathrm{SYM}}$ metric naturally holds the prosumers accountable for the induced additional losses due to the unbalance at prosumers' PoCs. Next, $\mathrm{RM}_{\mathrm{SYM}}$ at FEED,PCC ($P^{SYM}_{FEED,PCC}$) represents the total system losses, while $\mathrm{RM}_{3\mathrm{ph}}$ ($P^{3ph}_{FEED,PCC}$) only registers the losses belonging to the sub-grid, which are comparable to Case 8.

In Case 10, the sum of $P^{SYM}_{PRO1,PoC} + P^{SYM}_{PRO2,PoC}$, which is equal to $P^{SYM}_{FEED,PCC}$, gives the total system losses, ΔP_{act}, and it consists of additional losses in the community sub-grid solely, as caused by the unbalanced full exchange of energy between the prosumers. Thus, again, the feeder only covers the sub-grid losses, which are registered equally by all the metrics in the FEED,PCC and are accounted correctly by the $\mathrm{RM}_{\mathrm{SYM}}$ metric in the prosumers' PoCs. Conversely, the $\mathrm{RM}_{\Sigma 1\mathrm{ph}}$ in PRO1/PRO2,PoC delivers the information about the import and export in the phases. Thus, $\mathrm{RM}_{3\mathrm{ph}}$ might be regarded as registering zero in both registers at both prosumers' PoCs. Therefore, the network losses cannot be linked with these RMs.

In Case 11, PRO1 uses the DS as an interphase balancer and consequently causes a voltage unbalance at FEED,PCC (as in Case 5 of section V). PRO2 (the customer with a 3-ph symmetric passive resistive load) inherits the voltage unbalance at PRO2,PoC, thus absorbing the unbalanced power. However,

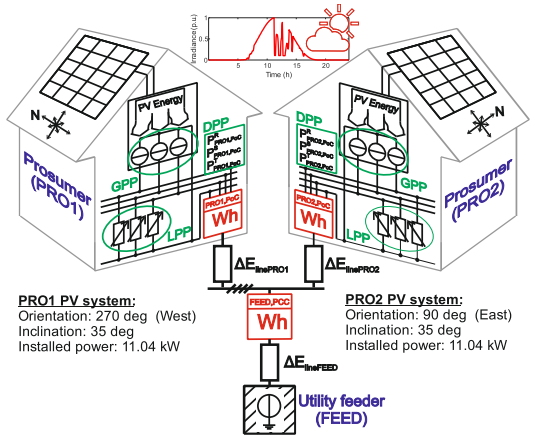

FIGURE 11. Realistic model of a system with two prosumers connected to adjacent branches of a community sub-grid during a typical day.

RM_{SYM} does not hold PRO2 to account for any additional losses (compared to the individual metrics in PRO2,PoC in TABLE 1.), which again confirms the fairness of the RM_{SYM} metric, because the 3-ph passive resistive load is symmetric.

VII. DAILY POWER PROFILE OF THE TWO PROSUMERS

This section discusses how a system with two prosumers was investigated by means of the realistic parameterization of the model in Fig. 2 during a typical day (Fig. 11). The day active power profile (DPP) of each prosumer consists of three series (3-ph) of consecutive 1 s steady states (i.e., 86 400 energy increments for each phase), while the DPP is the superposition of the generator power profile (GPP) and load power profile (LPP), neither of which exceeds 3.68 kW per phase.

The LPP was obtained by juxtaposition over the time of pseudo-randomly switched virtual appliances with random power in the range of 5–3680 W and a constant base load of 200 W in each phase independently. The pseudo-random part of the LPP is generated using a Beta distribution with parameters $\alpha = 0.4$ and $\beta = 4$. The appliance turn-on time is inversely proportional to the appliance power. Furthermore, the energy consumed in the variable/random part of the LPP is calculated with respect to the standard nationwide load profiles on an hourly basis [29]. The base load of the LPP represents approximately 10% of the prosumers' daily consumption. In total, the daily consumed energy per prosumer is 47.58 kWh for PRO1 and 47.96 kWh for PRO2.

The GPP represents the output of a 3-ph symmetrical inverter (i.e., the active power evenly distributed among phases), whereby the daily energy yield produced is equal to the daily energy consumed by the prosumer (47.58 kWh for PRO1 and 47.96 kWh for PRO2). The GPP reaches 3.68 kW at a maximum per phase (corresponding to the 11.04 kW rated output of the inverter), and the shape is defined by ideal solar irradiation affected by random cloud shading (factor in range of 0.05–1), with the same values for both prosumers. The shading factor is generated based on a normal distribution, smoothed by the spline average, and updated every 10 min. The resulting normalized irradiance curve is presented in Fig. 11. However, the prosumers' GPPs are shifted and modified in time because the PV panels of PRO1 are oriented to the west, while those of PRO2 to the east.

In addition, a reference balanced DPP is simulated. It relies on a balanced LPP (obtained in consonance with the above mentioned specification) using the same power profile for all three phases. It makes it possible to express the daily additional losses due to the unbalance (ΔE_{add}).

A. DAILY REGISTERED ENERGY

The series of energy increments (measured average active power values during consecutive 1 s steady states) registered by the metrics in the import and export registers in nodes PRO1,PoC, PRO2,PoC, and FEED,PCC during the day are shown in Fig. 12. The detail in Fig. 12D) focuses on a time period between 6:48 a.m. and 8:12 a.m., when the RM_{3ph} and RM_{SYM} metrics register significantly different values from $RM_{\Sigma 1ph}$. This is the interval when the prosumers transit from predominantly consumption to predominantly production. It has to be noted that the registers of RM_{3ph} and RM_{SYM} are disjunctive by definition (see (3), (4), and (8), (9)); this means that one of them (Imp or Exp) is always zero in each measuring window. Therefore, the Imp and Exp registers of RM_{3ph} and RM_{SYM} are summed for the sake of simplicity in Fig. 12.

The energy values registered within the test day in the export and import registers in the system nodes are shown in Fig. 13A as percentages of the values registered by $RM_{\Sigma 1ph}$, which had the highest amounts for both Imp and Exp. The differences for both RM_{3ph} and RM_{SYM} are in the range of 3–4% of the values for $RM_{\Sigma 1ph}$. This deviation is considered non-negligible: 1) it is beyond the accuracy of most of the LV revenue meters (up to 2% or 1%), and 2) it is comparable to the general losses in LV DSs (~3%). RM_{SYM} registers higher energy than RM_{3ph} in Imp and lower energy in Exp, and the differences reflect the additional losses (ΔE_{add}) in the DS due to the randomly changing unbalance (compare the first and second columns in Fig. 13B). The additional losses are ~25% of the total losses (ΔE_{act}), and they are evenly distributed among the DS lines (see $\Delta E_{linePRO1}$, $\Delta E_{linePRO2}$, and $\Delta E_{lineFEED}$, which refer to lines from nodes PCC to PRO1,PoC; PCC to PRO2,PoC; and FEED,PoC to PCC, respectively).

It can be concluded that if the prosumers export and import energy according to the stochastic deployment of the loads and stochastically changing irradiance, the long-term difference between the examined metrics can be expected to be approximately 4%. This value could be even higher if the situations with consumption in one phase and production in the other phase represent a significant percentage of the operating time. The value of 4% for the registered energy reflects the losses in the DS. Thus, it is

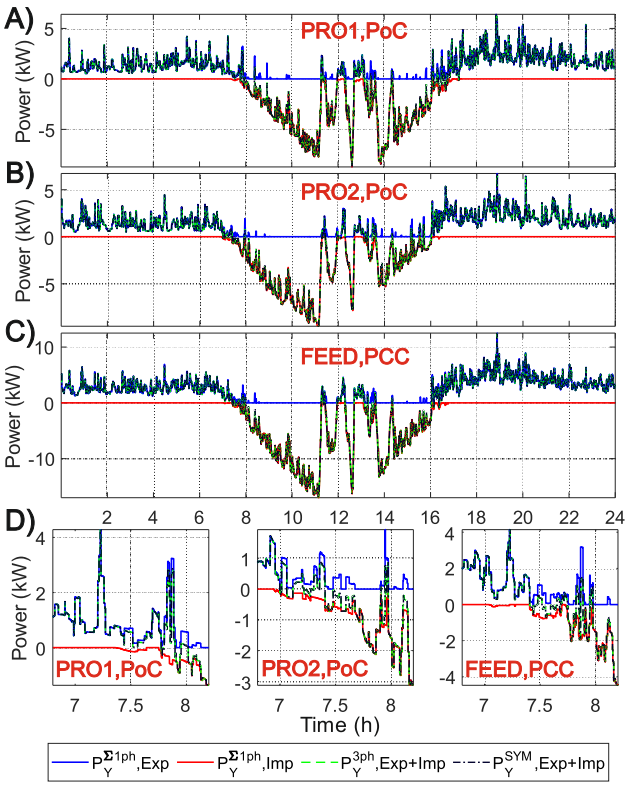

FIGURE 12. One-second average power profiles at A) PRO1,PoC, B) PRO2,PoC, C) FEED,PCC; where D) shows the detailed view. The Imp and Exp registers are summed for RM_{3ph} and RM_{SYM}.

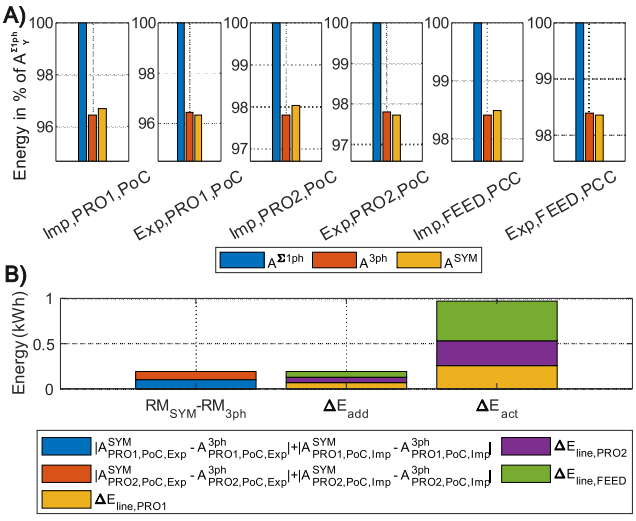

FIGURE 13. A) Import and export registers at measurement points PRO1,PoC; PRO2,PoC, and FEED,PCC; and B) additional losses and total system losses.

not negligible from the perspective of assigning the cost and efficiency of the energy distribution. However, 4% of the registered energy is not significant in the context of splitting the cost of active energy generation in power plants.

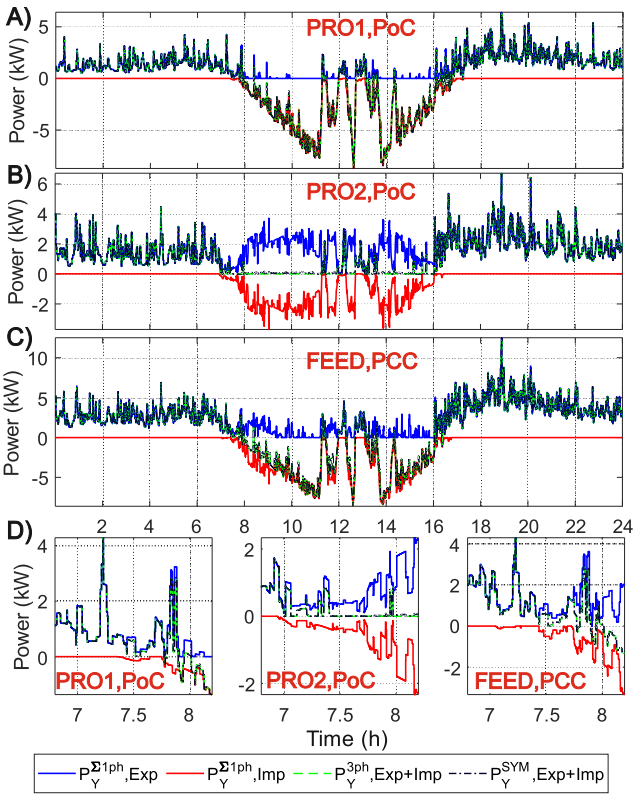

FIGURE 14. One-second average power profiles (one balancing prosumer case) at A) PRO1,PoC; B) PRO2,PoC; C) FEED,PCC; where D) shows the detailed view. The Imp and Exp registers are summed for RM_{3ph} and RM_{SYM}.

B. DAILY REGISTERED ENERGY WITH ONE BALANCING PROSUMER

The LPP and GPP, given by emulating the natural stochasticity, might be affected by the intentional energy diverting employed by prosumers. Practically, the prosumers might be motivated to provide zero export, i.e., a zero value in the export register of RM. However, if the RM implements either RM_{3ph} or RM_{SYM}, this zero in the export register might be accompanied by a power unbalance at the PoC (see Case 5 in TABLE 1.). Let us consider an example: PRO2 from Fig. 11 is equipped with an energy diverter, with the goal of a zero value in the export register of RM_{3ph}, which implements the same diverting control and logic as commercial devices. For instance, performing as a variable resistive load with a rated power value of 3.68 kW in phase R and constant resistive loads with the same rated power values in phases S and T, both switched as a cascade [13]. The resulting power profiles at each PoM for all considered and monitored metrics and registers are shown in Fig. 14. Fig. 14D shows a portion of the time interval from 6:48 a.m. to 8:12 a.m. when significant differences between $RM_{\Sigma 1ph}$ and the other metrics appear. Obviously, the difference in the daily registered energy is also significant, as summarized in Fig. 15A. The difference between $RM_{\Sigma 1ph}$ and RM_{3ph} at PRO2,PoC is 29.8% of $RM_{\Sigma 1ph}$ in its import register and

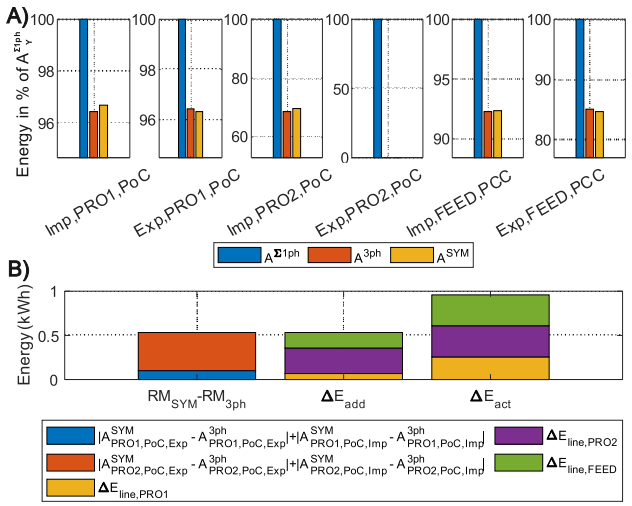

FIGURE 15. A) Import and export registers at measurement points PRO1,PoC; PRO2,PoC; and FEED,PCC; and B) additional losses and total system losses with one balancing prosumer.

100% in the export register, which leads to a difference of 7.7% in the import register and 15.3% in the export register between the metrics at FEED,PCC.

Similar to section VII-A, the difference between RM_{SYM} and RM_{3ph} at PRO1/PRO2,PoC reflects the additional losses due to the unbalance ΔE_{add} (compare the first and second bars in Fig. 15B). Those additional losses are mostly introduced by the diverting device in the PRO2 installation (see the purple part of the second bar in Fig. 15B). When comparing Fig. 15B and Fig. 13B, it can be noticed that the losses due to the unbalance, ΔE_{add}, are considerably higher with the diverter at PRO2 ($\sim$50% of ΔE_{act}), while the absolute value of the total losses, ΔE_{act}, does not differ essentially ($\sim$1 kWh in both situations). Furthermore, the total losses in the sub-grid ($\Delta E_{line,PRO1}+\Delta E_{line,PRO2}$) are slightly higher in Fig. 15B than in Fig. 13B (compare the sub-bars of ΔE_{act}).

VIII. CONCLUSION

This paper addressed equitable revenue metering in a low-voltage distribution system integrating prosumers, which may additionally be involved in an energy community sub-grid (part of the DS). Because of the presence of generation and simultaneous consumption, bidirectional and unbalanced active energy flows are invoked, significantly changing the paradigm of the energy flow in the DS and affecting the concept of energy measurement and registration. In contrast to standard revenue meter metrics, which sort the active energy increments measured in individual phases into registers ($RM_{\Sigma 1ph}$ and RM_{3ph}), it has been examined and compared an alternative metric based on the active energy carried by symmetrical components (RM_{SYM}). Basically, $RM_{\Sigma 1ph}$ implicitly gives information about the system occupancy, i.e., how much energy is transferred through the point of measurement. On the other hand, the RM_{3ph} metric provides information about the energy balance of the downstream system (e.g., the prosumer installation). Moreover, RM_{SYM} accounts for the additional losses due to an unbalance in the upstream system.

Employing extensive simulations with one and two prosumers operating in a representative DS, we demonstrated that the $RM_{\Sigma 1ph}$ and RM_{3ph} metrics currently deployed in three-phase revenue meters may fail to fairly charge unbalanced prosumers for their use of the distribution system as an inherent phase-to-phase balancer. On the other hand, it was proven that adopting the RM_{SYM} metric would enable fairer billing within the community. Consistent conclusions were also reached if the prosumer energy management employs intentional balancing. Furthermore, it was verified that the increase in the system losses caused by an unbalanced prosumer can be quantified by means of negative and zero sequence power values measured at his point of connection with a good approximation.

The main contribution of the paper is a detailed and systematic comparison of the methods used for the measurement and sorting of energy into registers in RMs to support the ongoing discussions about fair metering within future energy communities. Ongoing research activities are focused on the experimental validation of the proposed considerations and on the design of a power balancer based on positive sequence active power.

REFERENCES

[1] M. Rezaeimozafar, R. F. D. Monaghan, E. Barrett, and M. Duffy, "A review of behind-the-meter energy storage systems in smart grids," *Renew. Sustain. Energy Rev.*, vol. 164, Aug. 2022, Art. no. 112573, doi: 10.1016/j.rser.2022.112573.

[2] Y. Chen, M. Tanaka, and R. Takashima, "Energy expenditure incidence in the presence of prosumers: Can a fixed charge lead us to the promised land?" *IEEE Trans. Power Syst.*, vol. 37, no. 2, pp. 1591–1600, Mar. 2022, doi: 10.1109/TPWRS.2021.3104770.

[3] A. I. Nikolaidis and C. A. Charalambous, "Hidden financial implications of the net energy metering practice in an isolated power system: Critical review and policy insights," *Renew. Sustain. Energy Rev.*, vol. 77, pp. 706–717, Sep. 2017, doi: 10.1016/j.rser.2017.04.032.

[4] F. Bignucolo, R. Caldon, M. Coppo, and R. Turri, "Effects of distributed generation on power losses in unbalanced low voltage networks," in *Proc. IEEE Power Energy Soc. Gen. Meeting (PESGM)*, Aug. 2018, pp. 1–5, doi: 10.1109/PESGM.2018.8586092.

[5] B. Chen, L. Ye, T. Cui, and W. Bi, "Power loss analysis for low-voltage distribution networks with single-phase connected photovoltaic generation," in *Proc. 5th Int. Conf. Electric Utility Deregulation Restructuring Power Technol. (DRPT)*, Nov. 2015, pp. 1929–1934, doi: 10.1109/DRPT.2015.7432589.

[6] L. S. Czarnecki, "Comments on active power flow and energy accounts in electrical systems with nonsinusoidal waveforms and asymmetry," *IEEE Trans. Power Del.*, vol. 11, no. 3, pp. 1244–1250, Jul. 1996, doi: 10.1109/61.517478.

[7] J. N. Fidalgo, C. Moreira, and R. Cavalheiro, "Impact of load unbalance on low voltage network losses," in *Proc. IEEE Milan PowerTech*, Jun. 2019, pp. 1–5, doi: 10.1109/PTC.2019.8810710.

[8] D. Gallo et al., "Case studies on large PV plants: Harmonic distortion, unbalance and their effects," in *Proc. IEEE Power Energy Soc. Gen. Meeting*, Jul. 2013, pp. 1–5, doi: 10.1109/PESMG.2013.6672271.

[9] R. Carbone, R. Langella, and A. Testa, "Grid-connected photovoltaic plants: Energy account problems," Presented at the 102° Convegno Nazionale AEIT, Catania, Italia, Sep. 2009.

[10] *Electricity Metering Data Exchange—The DLMS/COSEM Suite—Part 6-1: Object Identification System (OBIS)*, document IEC 62056-6-1:2017, 2017.

[11] *IEEE Standard Definitions for the Measurement of Electric Power Quantities Under Sinusoidal, Nonsinusoidal, Balanced, or Unbalanced Conditions*, Standard IEEE Std 1459-2010, IEEE Std 1459-2000, Mar. 2010, pp. 1–50, doi: 10.1109/IEEESTD.2010.5439063.
[12] M. Raeber, A. Heinzelmann, and J. Oliapuram, "Analysis of a three-phase AC chopper with high power factor for the use in 'PV-to-heat' applications," in *Proc. 45th Annu. Conf. IEEE Ind. Electron. Soc.*, Oct. 2019, pp. 2319–2323, doi: 10.1109/IECON.2019.8926733.
[13] *Fronius OhmPilot*, Operating Manual, Fronius, Wels, Austria, 2018.
[14] J. Drapela, J. Moravek, L. Radil, and P. Mastny, "Performance of standard power/energy metric under fast changes in active energy flow direction," in *Proc. 19th Int. Conf. Harm. Quality Pow. (ICHQP)*, 2020, pp. 1–6, doi: 10.1109/ICHQP46026.2020.9177900.
[15] R. Carbone, R. Langella, and A. Testa, "On the billing of electrical energy flows at prosumers' busbar," in *Proc. 14th Int. Conf. Harmon. Quality Power (ICHQP)*, Sep. 2010, pp. 1–7, doi: 10.1109/ICHQP.2010.5625479.
[16] J. Moravek, J. Drapela, V. Wasserbauer, and P. Mastny, "Power quality issues related to power flow control in systems with renewable energy micro sources," in *Proc. 17th Int. Scientific Conf. Electric Power Eng. (EPE)*, May 2016, pp. 1–6, doi: 10.1109/EPE.2016.7521784.
[17] L. Feola, R. Langella, and A. Testa, "On the effects of unbalances, harmonics and interharmonics on PLL systems," *IEEE Trans. Instrum. Meas.*, vol. 62, no. 9, pp. 2399–2409, Sep. 2013, doi: 10.1109/TIM.2013.2270925.
[18] P. Gnacinski, "Windings temperature and loss of life of an induction machine under voltage unbalance combined with over-or undervoltages," *IEEE Trans. Energy Convers.*, vol. 23, no. 2, pp. 363–371, Jun. 2008, doi: 10.1109/TEC.2008.918596.
[19] L. Jiang, J. Meng, Z. Yin, Y. Dong, and J. Zhang, "Research on additional loss of line and transformer in low voltage distribution network under the disturbance of power quality," in *Proc. Int. Conf. Adv. Mechatr. Syst. (ICAMechS)*, 2018, pp. 364–369, doi: 10.1109/ICAMechS.2018.8507080.
[20] A. M. Blanco, J. Meyer, P. Schegner, R. Langella, and A. Testa, "Survey of harmonic current unbalance in public low voltage networks," in *Proc. 17th Int. Conf. Harmon. Quality Power (ICHQP)*, Oct. 2016, pp. 289–294, doi: 10.1109/ICHQP.2016.7783318.
[21] F. Moller and J. Meyer, "Survey of voltage unbalance and unbalanced power in German public LV networks," in *Proc. 20th Int. Conf. Harmon. Quality Power (ICHQP)*, May 2022, pp. 1–6, doi: 10.1109/ICHQP53011.2022.9808568.
[22] J. Meyer, F. Moller, S. Perera, and S. Elphick, "General definition of unbalanced power to calculate and assess unbalance of customer installations," in *Proc. Electric Power Quality Supply Rel. Conf. (PQ) Symp. Electr. Eng. Mechatronics (SEEM)*, Jun. 2019, pp. 1–6, doi: 10.1109/PQ.2019.8818268.
[23] S. Pajic and A. Emanuel, "Effect of neutral path power losses on the apparent power definitions: A preliminary study," in *Proc. IEEE Power Energy Soc. Gen. Meeting Convers. Del. Electr. Energy 21st Century*, Jul. 2008, pp. 517–523, doi: 10.1109/PES.2008.4596441.
[24] V. P. Brasil, J. Y. Ishihara, and A. L. F. Filho, "Fair power factor billing under unbalanced and nonsinusoidal voltage supply," *IEEE Access*, vol. 10, pp. 19301–19311, 2022, doi: 10.1109/ACCESS.2022.3151379.
[25] J. Klusacek, J. Drapela, and R. Langella, "Power symmetrical components as grid usage indicator for unbalanced prosumers," in *Proc. 20th Int. Conf. Harmon. Quality Power (ICHQP)*, May 2022, pp. 1–6, doi: 10.1109/ICHQP53011.2022.9808706.
[26] *Distribution System Operation Rules—Grid Code (PPDS, in Czech)*, Distrib. Grid Operators, Czech Regulatory Office, 2022.
[27] *Technical Connection Rules for Low-Voltage*, document VDE-AR-N 4100, 2019.
[28] R. Stiegler et al., "Survey of network impedance in the frequency range 2–9 kHz in public low voltage networks in AT/CH/CZ/GE," in *Proc. 25th Int. Conf. Electr. Distrib.*, 2019 pp. 1–5.
[29] *Consideration of Reference Impedances and Public Supply Network Impedances for Use in Determining the Disturbance Characteristics of Electrical Equipment Having a Rated Current ≤75 A Per Phase*, document IEC TR 60725, 2012.
[30] Czech Electricity and Gas Market Operator (OTE). (Jul. 15, 2022). *Normalized LP*. [Online]. Available: https://www.ote-cr.cz/en/statistics/electricity-load-profiles/computed-lp?set_language=en&date=2022-09-13

JAN KLUSACEK (Student Member, IEEE) received the M.Sc. degree in electrical power engineering from the Brno University of Technology, Brno, Czechia, in 2020, where he is currently pursuing the Ph.D. degree with dissertation topic "Definition and Measurement of Electrical Power Components in Future Distribution Systems."

His research interests include power measurement, power quality in active distribution systems, power converters, and coordination of distributed generators.

JIRI DRAPELA (Senior Member, IEEE) received the M.Sc. and Ph.D. degrees in electrical power engineering from the Brno University of Technology, Brno, Czechia, in 1999 and 2006, respectively.

He is currently with the Brno University of Technology as a Full Professor of power systems and a Team Leader of the Power Quality Research Group. His research interests include power quality and power network conducted disturbances, especially immunity, emission of electrical appliances, and power quality measurement techniques.

ROBERTO LANGELLA (Senior Member, IEEE) was born in Naples, Italy, in March 1972. He received the Laurea degree in electrical engineering from the University of Naples, Italy, in 1996, and the Ph.D. degree in electrical energy conversion from the University of Campania Luigi Vanvitelli, Italy, in 2000.

He is currently a Full Professor of electrical power systems with the University of Campania Luigi Vanvitelli. He is the Chair of the IEEE PES TF on Harmonic Modeling, Simulation, and Assessment.